Energy range of hadronic calorimeter towers and cells for high-p_T jets at a 100 TeV collider

S.V. Chekanov[a,*], J. Dull[b]

[a] *HEP Division, Argonne National Laboratory, 9700 S.Cass Avenue, Argonne, IL 60439, USA.*
[b] *St. Olaf College, 1520 St. Olaf Avenue, Northfield, MN, 55057, USA.*

Abstract

This paper discusses a study of tower and cell energy ranges of a hadronic calorimeter for a 100 TeV *pp* collider. The dynamic energy ranges were estimated using Standard Model jets with transverse momenta above 20 TeV. The simulations were performed using the PYTHIA Monte Carlo model after a fast detector simulation tuned to the ATLAS hadronic calorimeter. We estimate the maximum energy range of towers and cells as a function of lateral cell sizes for several extreme cases of jet transverse energy.

Keywords: hadronic calorimeter, dynamic range, Monte Carlo, FCC, format, IO, LHC

1. Introduction

The Future Circular Collider (FCC) is a proposed 80-100 km long ring that would collide protons at 100 TeV. A massive experiment like this would need a detector that could measure very high energies. For example, collisions at 100 TeV will produce hundreds of Standard Model jets with transverse momentum $p_T > 20$ TeV[1], while many models beyond the Standard Model can lead to even larger number of jets above 20 TeV. This means that the calorimeter system of an FCC detector must be able to handle large energy depositions. The dynamic range of towers and cells of the hadronic calorimeter of this future detector must be well understood in order to set a stage for technology choices of future calorimeters.

The current calorimeters at the LHC are designed to measure jets with transverse momenta up to 4 TeV. The dynamic range of cells of a typical calorimeter at the LHC is about 10^4, spanning the energy range of $0.2-1500$ GeV for the ATLAS Tile calorimeter [1],[2]. The lowest energy of 0.2 GeV is typically needed for muon reconstruction, while the upper value of this range is set by high-p_T jets. It is clear that the dynamic range of a calorimeter that is designed to measure jets above 20 TeV should substantially be extended.

*Corresponding author

Email addresses: chekanov@anl.gov (S.V. Chekanov), dull@stolaf.edu (J. Dull)

[1] We assume the cross section of 0.02 fb^{-1} for the jet production with $p_T(jet) > 20$ TeV and with an integrated luminosity of 10 ab^{-1}

In order to explore the maximum dynamic range of such a calorimeter, we use the HepSim repository [3] with Pythia8 predictions [4, 5], and the Delphes fast simulation program [6] after a proper tune of this simulation to describe energy sharing between different layers of hadronic calorimeters. We discuss the expected dynamic range for high-luminosity LHC (HL-LHC), and then we will repeat this analysis for 100 TeV collision energies. In our discussion, we assume a "typical" hadronic calorimter that has an interaction length λ of the hadronic part of 80% of the total interaction length of the entire calorimeter, that consists of electromagnetic and hadronic sections.

2. Fast simulation

Fast detector simulation uses the Delphes framework which incorporates a tracking system, magnetic field, calorimeters, and a muon system [6]. Delphes simulates the calorimeter system by summing together cells to form "towers". The towers are divided to electromagnetic and hadronic towers. For the central analysis in this paper, we used towers of the size 0.1×0.1 in pseudorapidity (η) and the azimuth angle (ϕ). Such tower sizes correspond to the sizes of the ATLAS hadronic calorimeter, the so-called Tile calorimeter.

Preforming the study of cell dynamic range requires tuning Delphes to a full simulation of a hadronic calorimeter in order to reproduce the longitudinal energy profile of hadronic shower of jets. To tune Delphes towers to the Tile calorimeter, we assume that about 60% of charged particle energy is deposited in the hadronic section [7], and 40% in the electromagnetic section, while 100% of γ and π^0 energy is deposited in the electromagnetic section only. It should be pointed out that these fractions are set to be constant and do not depend on particle's momentum, since Delphes does not handle energy sharing between electromagnetic and hadronic parts of a calorimter.

To convert towers to the cells we must go a step further. In the case of the ATLAS calorimeter, about 50 ± 15% of a jet's energy inside the hadronic calorimeter is deposited to the first layer. This was determined by running a full detector simulation for the ATLAS calorimeter system [1]. In order to convert tower energies to the cell energies, a random scaling factor was applied to the tower energies using a Gaussian distribution with the standard deviation of 0.15.

3. Results

3.1. ATLAS-like calorimeter for HL-LHC

With Delphes correctly tuned, Standard Model dijet events were generated by PYTHIA8 Monte Carlo model. The truth-level samples were downloaded from the HepSim repository [3]. The jets are reconstructed using the anti-k_T algorithm [8] with a distance parameter of 0.4 using the FastJet package [9]. We select jets with $p_T > 3$ TeV and $\eta < 0.8$. In total, about 5,000 high-p_T events were considered for this study. Figure 1 shows that 10 ± 5 towers make up a $R = 0.4$ jet in the Delphes program.

If we consider whole towers to have a limited dynamic range of 1.2 TeV (1.5 TeV), then we find 70% (32%) of jets with at least one tower past this limit. For jets with $p_T > 4$ TeV, these percentages rise to about 75% and 60% respectively. However, these

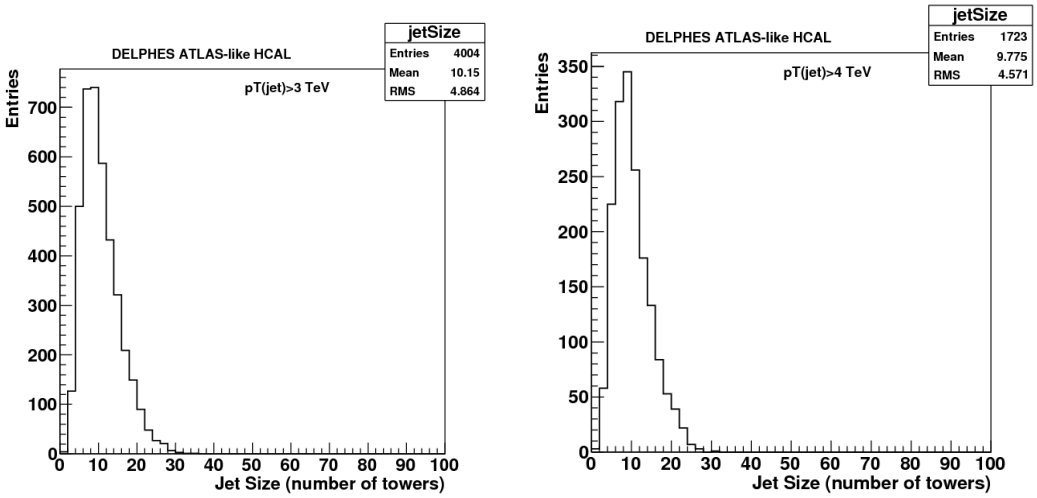

(a) (b)

Figure 1: Jet size distribution for the ATLAS detector. Size is determined by summing together all instances of there being a tower within a jet.

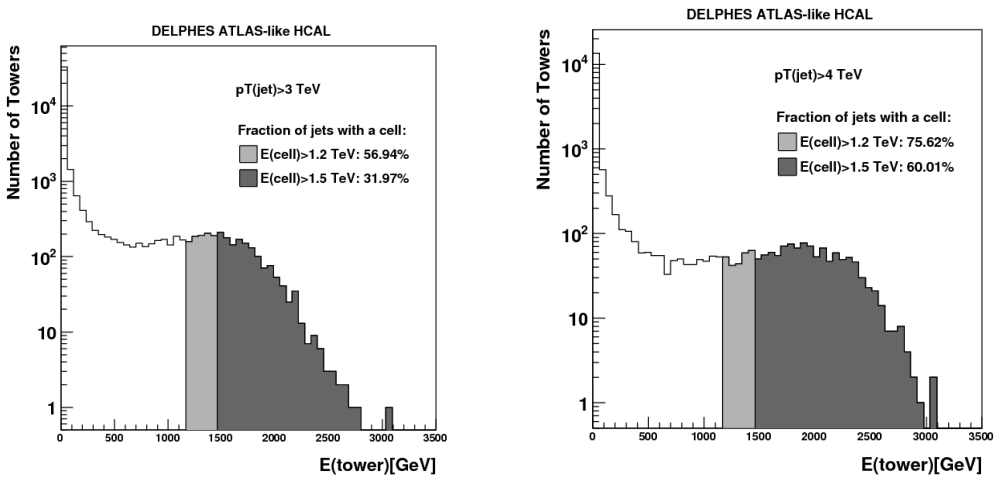

(a) (b)

Figure 2: Energy distributions of tower energy in ATLAS's TileCal for 14 TeV, Standard Model, dijet events trimmed to $p_T(jet) > 3$ TeV (a) and $p_T(jet) > 4$ TeV (b).

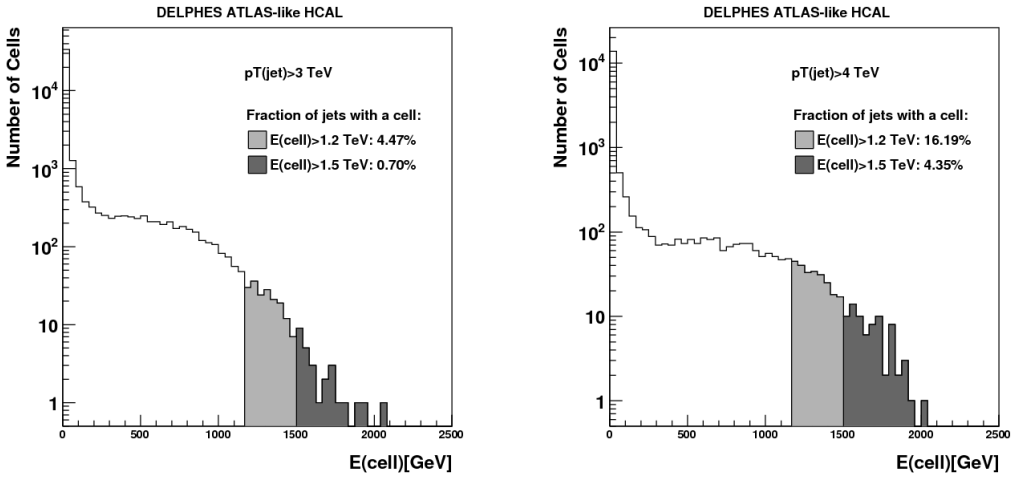

(a) (b)

Figure 3: Energy distributions of cell energy in ATLAS's TileCal for 14 TeV, Standard Model events trimmed to $p_T(jet) > 3$ TeV (a) and $p_T(jet) > 4$ TeV (b).

fractions decrease when individual cells are simulated. Figure 3 shows the fraction of jets affected by cell limits of 1.2 and 1.5 TeV drop to about 5% and 1%, respectively. Since multiple cells make up one tower, a single cell will never measure as much energy as a tower does. Thus, a cell is much less likely to saturate. The obtained limits are similar to those anticipated for the hadronic-calorimeter cells after for the ATLAS phase-II [2].

It should be noted that this simulation presents an optimistic view of these jet fractions. This study makes the assumption that all energy of hadrons in the hadronic part of a calorimeter system is fixed to 60%, as discussed before. Since Delphes does not correct for energy-dependent effects of longitudinal propagation of particles. Hence, the actual jet fractions may be higher than the values presented here. Nevertheless, the simulated numbers are found to be close to those found by running a full simulation of the ATLAS detector.

3.2. ATLAS-like calorimeter for 100 TeV collisions

After studies of HL-LHC, we will turn to jets to be produced at a 100 TeV collider. As before, we will use the Delphes simulation tuned to the ATLAS-like hadronic calorimeter as described in the previous sections. The truth-level samples with 100 TeV collisions were downloaded from the HepSim repository [3]. The jets are reconstructed using the anti-k_T algorithm as discussed before. For our studies, we will use jets with $p_T > 20$ TeV and $\eta < 0.8$.

Figure 6(a) shows that nearly half of all high-p_T jets have at least one cell of size 0.1×0.1 above 5 TeV. If cells are limited to the 10 TeV range, then only about 5% of jets have a saturated cell reading. These numbers, 5 and 10 TeV, are used as our initial guesses to illustrate the maximal dynamic range anticipated for a 100 TeV machine.

The lateral cell sizes of a calorimeter for a 100 TeV collider still need to be determined by looking at different physics cases. One possible option is to reduce the cell

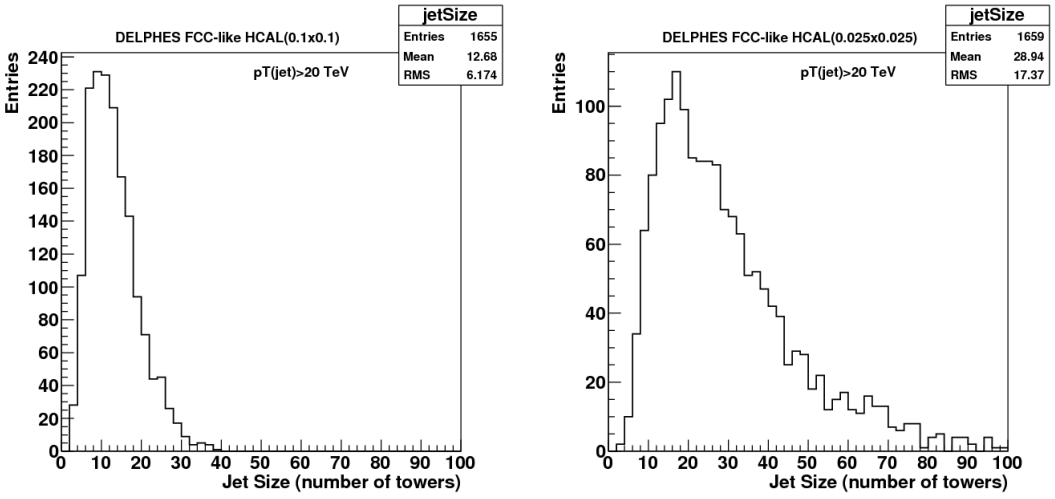

(a) (b)

Figure 4: Jet size distribution for a FCC detector. When the tower size decreases from 0.1×0.1 (a) to 0.025×0.025 (b) the number of towers found in a jet increases. This helps reduce the dynamic range of tower and cells.

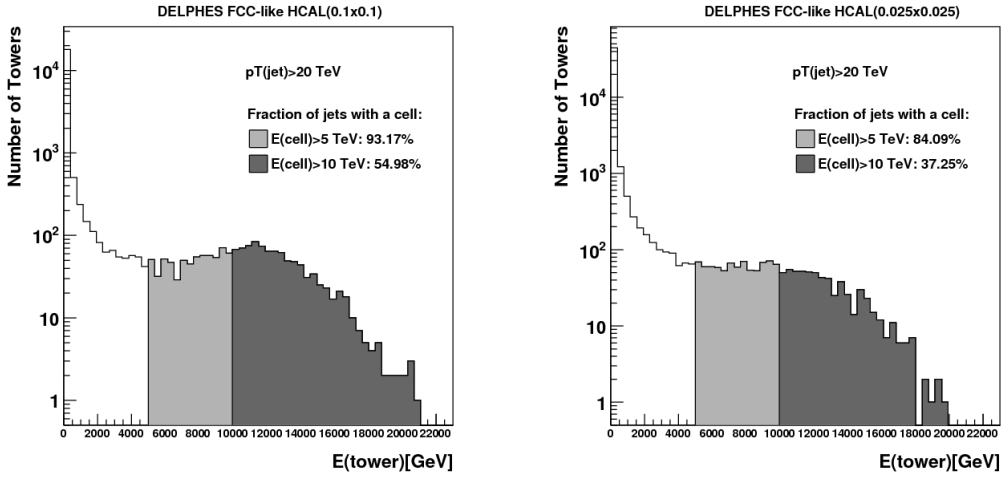

(a) (b)

Figure 5: Energy distributions of tower energy in Tile calorimeter for a FCC detector using cell sizes of 0.1×0.1 (a) and 0.025×0.025 (b). These figures show the results for Standard Model, 14 TeV events trimmed to $p_T > 20$ TeV.

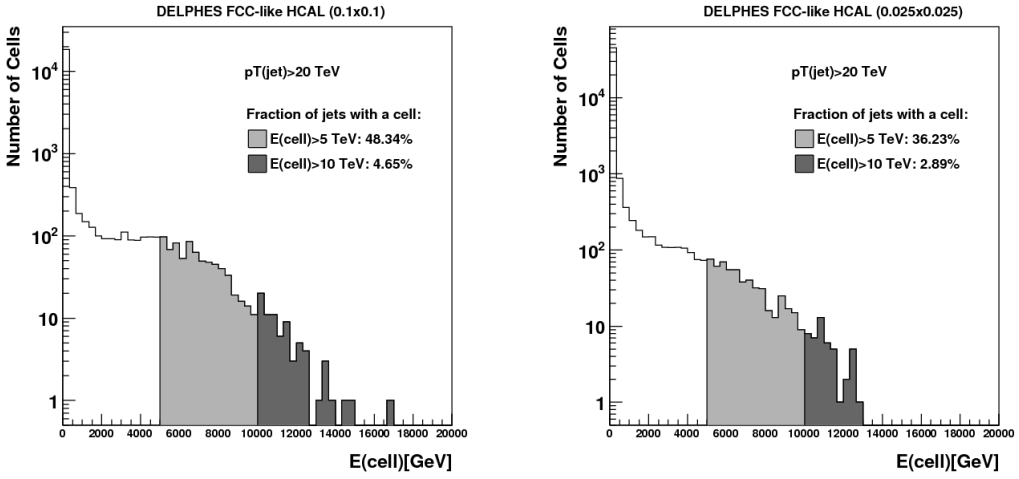

(a) (b)

Figure 6: Energy distributions of cell energy in TileCal for a FCC detector using cell sizes of 0.1×0.1 (a) and 0.025×0.025 (b). Standard Model, dijet, 14 TeV events trimmed to $p_T > 20$ TeV.

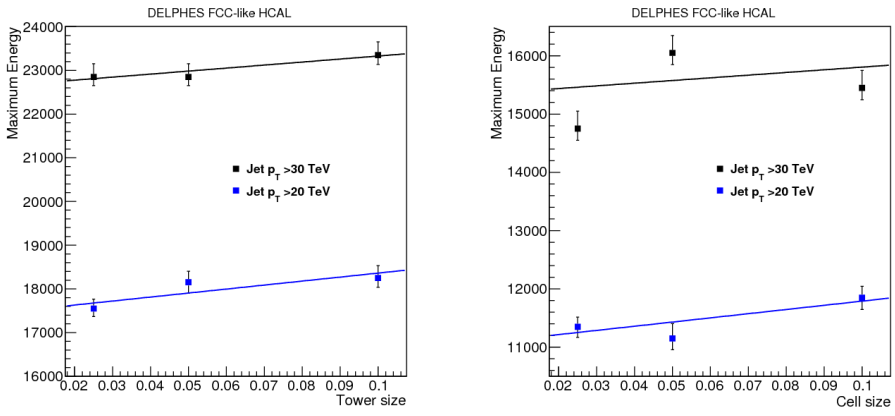

(a) (b)

Figure 7: Maximum value of energy seen by towers (a) and cells (b) for varying tower and cell sizes. We define maximum energy as the energy range that fully contains 99% of SM jet towers (or cells).

Fit Line ($MaxEnergy = p_1 \cdot E + p_0$)	Slope (p_1)	Constant (p_0)
Tower: $p_T(jet) > 30$ TeV	$(6.89 \pm 3.89) \cdot 10^3$	22600 ± 2610
Tower: $p_T(jet) > 20$ TeV	$(9.13 \pm 4.76) \cdot 10^3$	17400 ± 2820
Cell: $p_T i(jet) > 30$ TeV	$(4.59 \pm 5.50) \cdot 10^3$	15300 ± 340
Cell: $p_T i(jet) > 20$ TeV	$(7.17 \pm 3.66) \cdot 10^3$	11100 ± 240

Table 1: Parameters of the fit lines in Fig. 7 for maximum energy vs. tower/cell size. These values can be used to estimate the maximum energy range for various tower or cell size.

size by a factor four, i.e. to 0.025×0.025. With this geometry of cells, four cells would take the place of a single cell, allowing the four cells to "share" deposited energy.

The jet size distributions for the FCC detector are illustrated in Fig 4. For a tower division of 0.025×0.025, we find that the jets double in size compared to a detector with a tower size of 0.1×0.1. If twice as many cells make up a jet, we can expect that the energy range of those smaller cells wound not have to be as high. Figure 6(b) shows the result of such a simulation. The fraction of jets with a cell above 5 TeV decreased from 48% to 36%. A reduction also occurs in the 10 TeV case. Figure 5 shows the results for 5 and 10 TeV limits on towers, rather than cells. We again see a decrease in affected jets when tower size decreases. Thus, as the size of the detector cells (or towers) are made smaller the dynamic range decreases as well.

The decrease of the dynamic range on the lateral cell sizes is best illustrated in Fig. 7. The data on this figure shows the maximum energy of cells (or towers) that fully contains 99% of jet energy.

For jets with $p_T > 20$ TeV, as the cell (or tower) size increases the maximum energy seen by that cell increases too. At these energies, only 1% of jets have at least one cell (or tower) above the energy value. Figure 7 also shows the simulation results for jets with $p_T > 30$ TeV. At this energy level, the positive correlation between cell size and maximum energy is still present. With the fit line of Fig. 7, we can extrapolate to smaller or larger cell sizes and use maximum energy value to determine the necessary cell parameters for future calorimeter systems. The parameters for the fit lines can be found in Table 1.

4. Conclusion

This paper discusses the energy range of calorimeter towers and cells for HL-LHC and for a future hadronic calorimeter at a 100 TeV collider. We used a fast detector simulation in which energy sharing between electromagnetic and hadronic parts are tuned to the ATLAS detector. In addition, for calorimeter cells, we assumed that about 50% of total energy of the hadronic calorimeter will be deposited in the first layer of this calorimeter, i.e. in cells closest to the interaction point.

It was shown that about 4-5% (1%) of jets with $p_T > 3$ TeV will lose p_T in reconstruction due to the present dynamic range of ATLAS hadronic calorimeter (limits of 1.2 and 1.5 TeV). For 100 TeV pp collisions, the dynamic range should be extended to 18 TeV (towers) and 12 TeV (cells) for jets with $p_T > 20$ TeV, which will be rather common for 100 TeV collisions. This estimate assumes a similar lateral segmentation,

energy sharing between electromagnetic and hadronic calorimeters, and similar fraction of energy contributing to the first layer of hadronic calorimeter as for ATLAS. We have calculated how the maximal energy range decreases with decrease of cell sizes. These studies can be used to extrapolate the dynamic range values to smaller cell sizes. It should be noted that a provision for 30 TeV jets can be considered in the case of high-p_T jet physics or exotic long-lived jets that deposit most of their energy in regions close to the surface of the calorimeter.

Despite the fact that the fast simulation was tuned to reproduce the full simulation of the ATLAS calorimeter, it should be noted that the approximate nature of these calculations should fully be recognized when talking about 20-30 TeV jets. The quoted numbers are likely to be on the optimistic side, since the energy fraction of hadrons in a hadronic calorimeter should be energy dependent. At present, this effect cannot be simulated with a fast simulation. Nevertheless, we believe the obtained results can be used in early determination of the design options for a future hadronic calorimeter, but should later be checked when a full simulation become available.

Acknowledgements

We thank J. Proudfoot for discussion. The submitted manuscript has been created by UChicago Argonne, LLC, Operator of Argonne National Laboratory ("Argonne"). Argonne, a U.S. Department of Energy Office of Science laboratory, is operated under Contract No. DE-AC02-06CH11357.

References

[1] G. Aad, et al., Readiness of the ATLAS Tile Calorimeter for LHC collisions, Eur. Phys. J. C70 (2010) 1193–1236. arXiv:1007.5423, doi:10.1140/epjc/s10052-010-1508-y.

[2] F. Tang, et al., Design of the Front-End Readout Electronics for ATLAS Tile Calorimeter at the sLHC, IEEE Transactions on nuclear science 60 (2013) 018.

[3] S. Chekanov, HepSim: a repository with predictions for high-energy physics experiments, Advances in High Energy Physics 2015 (2015) 136093, available as http://atlaswww.hep.anl.gov/hepsim/. arXiv:1403.1886.

[4] T. Sjostrand, S. Mrenna, P. Z. Skands, PYTHIA 6.4 Physics and Manual, JHEP 05 (2006) 026. arXiv:hep-ph/0603175.

[5] T. Sjostrand, S. Mrenna, P. Z. Skands, A Brief Introduction to PYTHIA 8.1, Comput. Phys. Commun. 178 (2008) 852–867. arXiv:0710.3820, doi:10.1016/j.cpc.2008.01.036.

[6] J. de Favereau, et al., DELPHES 3, A modular framework for fast simulation of a generic collider experiment, JHEP 1402 (2014) 057. arXiv:1307.6346, doi:10.1007/JHEP02(2014)057.

[7] Y. Hernandez, The ATLAS Tile Calorimeter performance at LHC, Nucl. Instr. and Meth. in Phys. Res. 718 (2013) 83, proceedings of the 12th Pisa Meeting on Advanced DetectorsLa Biodola, Isola dElba, Italy, May 20 26, 2012.

[8] M. Cacciari, G. P. Salam, G. Soyez, The Anti-k(t) jet clustering algorithm, JHEP 0804 (2008) 063. arXiv:0802.1189, doi:10.1088/1126-6708/2008/04/063.

[9] G. P. S. M. Cacciari, G. Soyez, FastJet user manualhttp://arxiv.org/abs/1111.6097 arXiv:1111.6097.